Agent-based modeling of commuters in dense urban metro trains to measure spread of COVID-19

ABSTRACT

Social distancing is a key strategy to minimize the spread of COVID-19. Social distancing is easier to follow outdoors and is more difficult indoors, especially in crowded metropolitan areas and particularly while in transit. Metro cities are essential for the functioning of economies, and urban public transportation networks are the heartbeat of economic activity. Public transportation systems are usually very densely packed and are a source of concern for disease transmission due to infeasibility of adequate social distancing. In this paper, we highlight the usefulness of city-scale agent-based simulators in studying a particular non-pharmaceutical intervention to manage urban commute in an evolving pandemic. We explore the potential impact of traveling in cohorts, a policy that can be used in addition to existing solutions like wearing masks and reducing crowding. To this end, we develop a multi-agent simulator in which commuters are modeled as independent agents. Specifically we focus on COVID-19 transmission via metro-trains network in Mumbai (one of the most crowded cities in the world and among the worst affected by the pandemic) using a city-scale simulation. We observe that cohort sizes of 15 and above, compared to no cohorts, have a significant impact in limiting the additional spread of the infection due to opening of urban metros.

1 INTRODUCTION

Covid-19 has been a tragic event with over 33 million cases and over a million fatalities all over the world, as on 30 September 2020. Most countries had enforced lockdowns to reduce mobility in varying capacity, and with varying degrees of success. Data so far shows that dense urban regions are more impacted than sparse rural regions both in terms of infections and fatalities. This has been attributed to higher interactions between individuals in urban areas.

Specifically in the case of India, a nation-wide lockdown led to over 70% drop in mobility. Mumbai, the economic hub of the country has the highest population density (over $32,300 \ people/km^2$). The metro rail system in Mumbai, called *locals*, had a daily ridership of over 8.2 million passengers before the lockdowns went into place. As of this writing, it is still to resume normal operations.

If interactions cannot be avoided in the locals, can they at least be localized and concentrated? For an infectious disease to spread, the total count of interactions, over a period of time, is not as important a factor as the the count of interactions between *distinct* pairs of individuals. This suggests the idea of *social bubbles* arising from individuals traveling in cohorts. We explore this idea in the context of policies of mass transit for achieving greater mobility without significant increase in disease transmission.

Figure 1: Pre-pandemic commuters waiting for local trains at a station in Mumbai.

Figure 2: Pre-pandemic crowded local train in Mumbai.

We take the notion of social bubbles a step further by studying an intervention policy that home quarantines cohort members whenever any member either tests positive for the disease or displays symptoms.

2 METHODOLOGY

We implement cohorts and cohorting strategies on top of a city-scale agent-based epidemic simulator developed in [9]. The agent-based simulator already models interactions in households, workplaces, schools, neighbourhoods, and communities. Cohorts are implemented as an additional interaction space related to transportation.

Very briefly, the agent-based simulator consists of two components: 1) a synthetic city generator and 2) a disease spread simulator that simulates the spread of the infection on the generated synthetic city. The synthetic city has as many agents as the population of the city of interest, with the following attributes for each agent:

- age
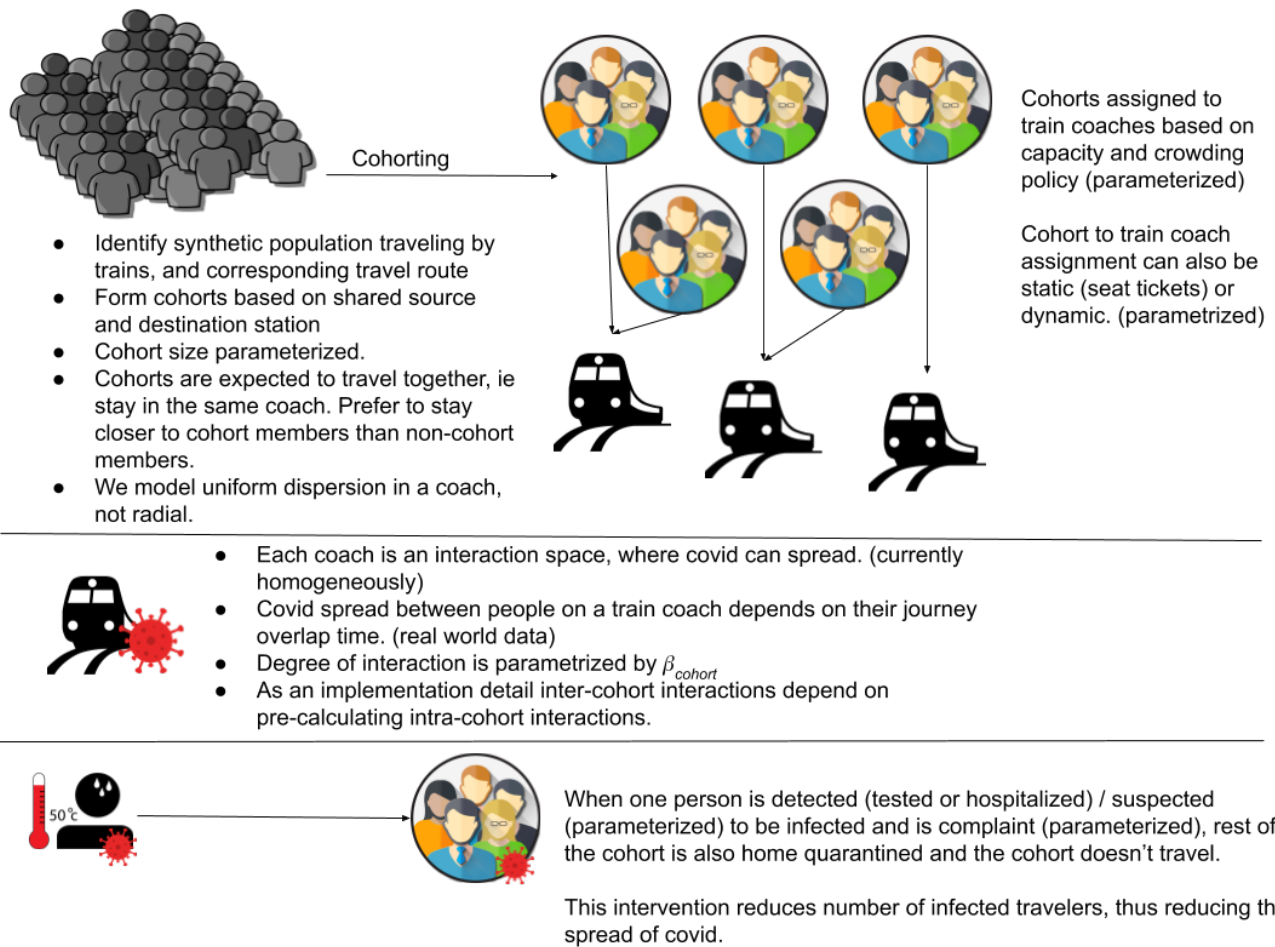- household to which the agent belongs including location

Figure 3: Schematic representation of our agent-based modeling of local trains.

- status – student, employed, or unemployed, based on the age and the census data on unemployed fraction in the city
- associated school/college or workplace
- if student, the class/grade/standard in the school for modelling closer association with students of roughly the same age
- if employed, an associated smaller project team at the workplace for modelling closer association with this subgroup
- the local neighbourhood associated with the household location
- a network of close friends and family to model frequent interactions with this group
- additional features related to transportation, does an office-going individual take the local or not

With all these attributes, agents constitute the nodes of a geo-spatial social network with mapped mobility. The disease simulator takes the generated network, a disease progression model, and simulates the spread of infection in the network. We expand on the modelling of the transport interaction space and cohorts in the next subsections.

2.1 Mumbai *locals* Dataset

We digitized the Mumbai Rail Map, and captured train line, train station, transit time between consecutive stations along a line, along with station latitude, longitude information. We restrict ourselves to the census city limits of Mumbai and Mumbai suburbs, to be consistent with agents being generated, and have 52 stations in the network. This data is used to pre-compute shortest travel route and corresponding time between any two stations across any line, making heuristic assumptions of transition time when the journey consists of multiple legs.

2.2 Cohorts

To model cohorts, in addition to the attributes mentioned above, we first determine if an office-going agent would take the train to go to work. For travel between home and workplace we optimize for travel time across various modes of travel, accounting for frequency and cost differential of road commute options compared to using *locals*, the expected speed of travel via road (21.6 km/h) along with geodesic to road detour index (value considered for Mumbai =

1.7), and multiple possible train stations an agent would consider as the primary commute stations both for home and workplace location. This allows us to know which agents take trains, and what route they follow. Our generated data shows that about 30% of the population takes train for daily workplace commute. Each cohort can have up to 3 legs in the journey (based on mumbai local network), where each leg represents travel along a single line of *locals* in a single coach.

Cohorts are assigned based on shared origin and destination stations. All individuals in the cohort are assumed to travel together while going to and coming back from office. Cohort size is parameterized, and the case of cohort size = 1 represents non-cohorting scenario. Each day cohorts get assigned to train coaches for their morning and evening commute. Disease transmission between individuals in coaches is uniformly dependent on their respective overlap time on the coach. Cohorts are accommodated in coaches taking into account, 1) the capacity of a coach, 2) allowed crowding factor (scaling factor of allowed maximum capacity that a coach can accommodate), and 3) occupancy between various stations along its route.

2.3 One-Off Travel

We model one-off travel for scenarios where individuals may not have a fixed daily commute destination, by separating travelers into 2 pools, those traveling in cohorts and those traveling individually. Each of these pools travels in separate coaches, and in practice could travel in different trains at different times to avoid infection spread at stations.

3 RESULTS

In this Section we discuss the simulation results obtained for various cohorting strategies and configurations. All simulations were done on a synthetic Mumbai city of population 12.4M covering the administrative area of Brihanmumbai Municipal Corporation (BMC). Based on the methodology described in Section 2.2, 3.74M individuals take trains for daily commute.

It is important to note that the daily positive counts is after taking into account interaction in other interaction spaces (household, office, neighbourhood, community) in addition to the transport interaction space. The plots thus show the impact of cohorting strategies on the progression of the *overall disease burden in the city*. Another feature of the simulator, is that it models spatial variance in population density and the associated increased contacts in slum areas, and therefore increased spread in these areas. A third important feature worth highlighting is that we model contact tracing and associated containment zones, which help contain the spread, this helps to not only match actual observed cases, but also model the benefit of contact tracing enabled case isolation in realistic way.

3.1 Executive Summary
- Cohorting can significantly reduce disease transmission. Larger cohort sizes are more effective.
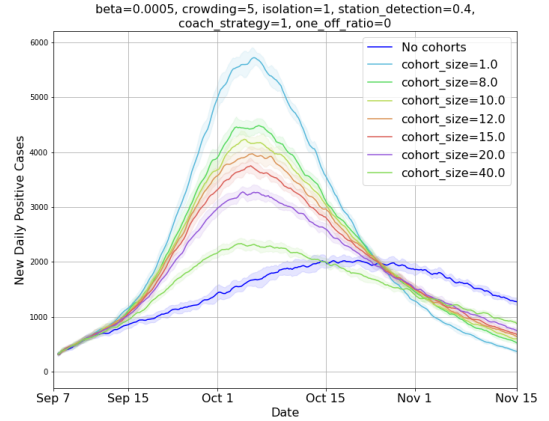

Figure 4: Cohort Size

- Effectiveness of cohorting entirely depends on effectiveness of isolation of cohorts if positive cases are detected or suspected in the cohort. Detection of symptomatic cases in stations is critical.
- Having fixed seats assignment (fixed coach for every cohort every single day) everyday doesn't have any perceivable impact on reducing disease transmission as compared to random seat assignment each day.
- Disease transmission is most sensitive to crowding in trains. But reducing crowding in trains can increase crowding at stations.
- One-off travel up to 10% will only show marginal increase in disease transmission, and even at 40% one-off travel, disease transmission can be significantly reduced by cohorting.
- While the model has focused on Mumbai metro rail system, we believe these findings are generally applicable to other public transit systems (like metros, buses).

3.2 Details
Figures 4 and 5 show the change in infection spread dynamics for various cohort sizes. We observe the following:
- Without isolation of cohorts, all cohorts have similar dynamics. Isolation here refers to home quarantining a cohort, when a member is suspected to be covid positive. By isolating a cohort we remove potentially asymptomatic carriers of the disease.
- If we impose restrictions and force cohorts to self isolate on detection of a case in the cohort, we observe reduction in disease spread, the reduction being larger for larger cohort sizes.
- Significant gain is observed only for larger cohort sizes.
- For cohort size 20, with and without cohort isolation, we observe peak daily rates of 3320 and 5999, respectively. Thus cohort sizes of 20 can have reasonable impact on reduction on disease spread via trains.

Figure 6 has daily positive cases for different crowding factors. Crowding factor of 1 indicates that the maximum number people
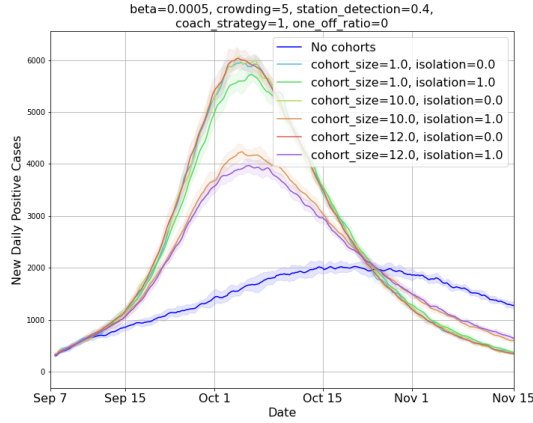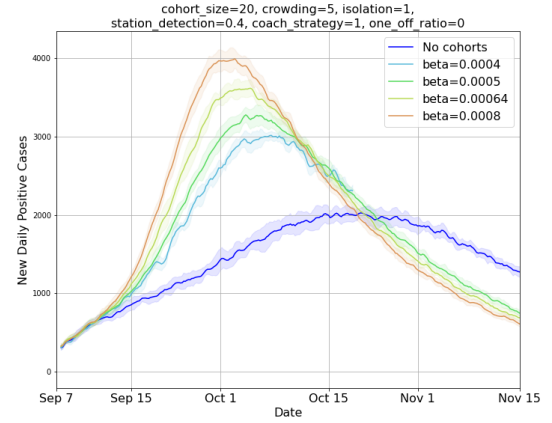
Figure 5: Cohort intervention policy
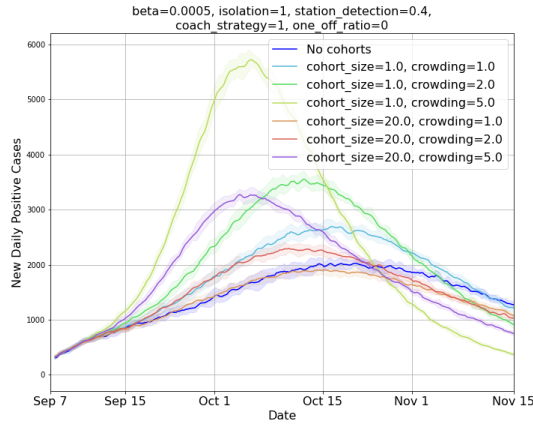

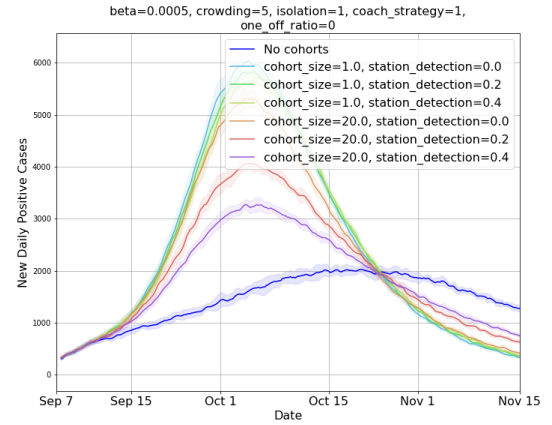Figure 7: β_{cohort}

Figure 6: Crowding

Figure 8: Symptomatic Detection at Station

allowed in a coach equals the seating capacity of the coach (100 in our simulations). We observe:

- Crowding factor has a significant effect on disease spread.
- Crowding factor of one without isolation has lower daily cases than crowding factor 2 with isolation, suggesting that reducing the crowding in trains by half has more impact than enforcing isolation of cohorts.
- The effect is more prominent when we increase crowding factor from 2 to 5.

In Figure 7 we plot daily positive cases for different β_{cohort}, the contact rate parameter for cohorts. Since we do not have a calibrated β value, it is important to study the robustness of the results to various β values. We observe:

- Higher β_{cohort} values cause higher disease transmission.
- Higher β_{cohort} values reach the peak earlier.
- We observe similar trend in the disease progression curves for different β values, suggesting that the qualitative results are robust to variations in β values.

In Figure 8 we study the impact of varying the detection probability of symptomatic individuals at stations. A detection triggers the isolation of the entire cohort. Detection of positive symptomatic individuals could potentially be achieved using thermal scanners at stations, and/or by employing random testing of individuals at stations. We plot daily positive cases for various detection probabilities and observe that:

- Increasing the detection probability from 0.2 to 0.4 reduces peak daily positive rate from 4088 to 3320 individuals per day.

In Figure 9 we study the impact of restricting cohorts to travel with the same set of cohorts on a daily basis against a much relaxed policy of allowing cohorts choose their train of choice and time of travel. The only restriction is that the cohorts should travel together. We observe the following:

- There is hardly any difference in the performance of the two strategies, suggesting that a strict association with a particular train and seat may not be warranted.
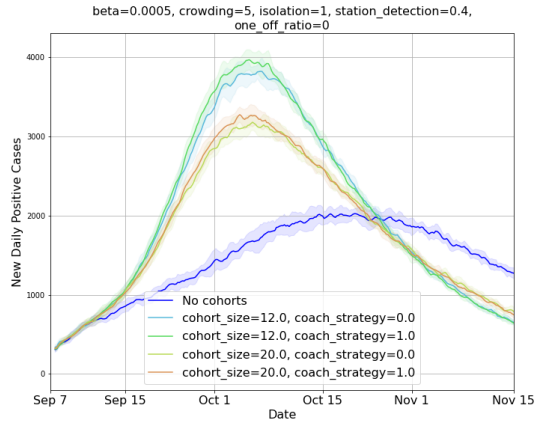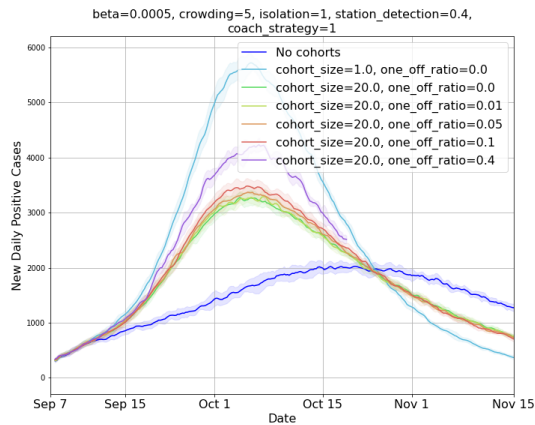
Figure 9: Cohort to coach mapping strategy

Figure 10: One-Off travel along side cohorts. Co-hort size of 1 represents 100% one-off travel

Figure 11: Peak Daily Positive Cases vs One-Off travel
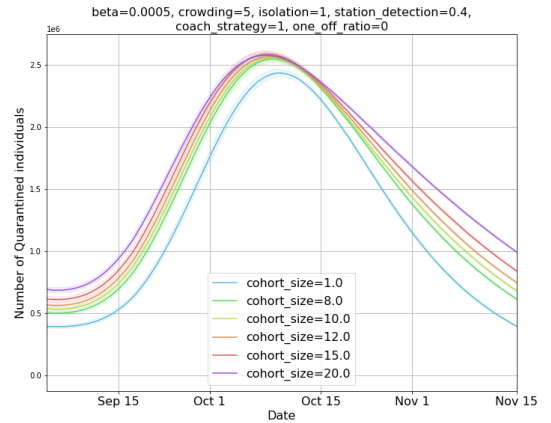
Figure 12: Daily Quarantined Individuals

Figure 13: Daily Quarantined Individuals in Co-horts

In Figure 10 we study the impact of allowing one-off travel along side cohorts. We assume one-off travellers use separate trains and thus avoid interacting with those in cohorts. We also assume that an individual can be one-off traveler or a cohort traveler but not both. We observe:

- If one-off travelers don't exceed 10% of overall travelers, they don't change disease dynamics significantly.
- Even with significant one-off travelers (40%), cohorts for the remainder of the population reduces disease transmission significantly.

In Figure 11 we see that the peak daily positive cases monotonically increases with increasing one off ratio.

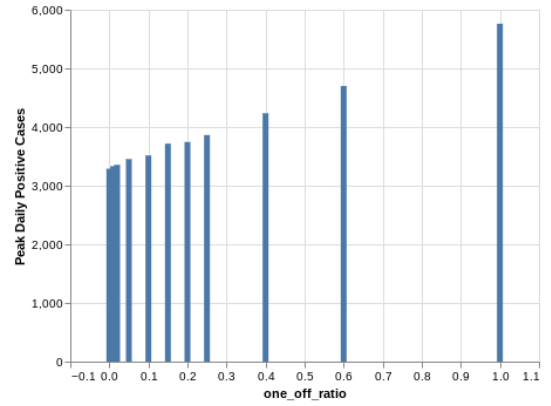In Figure 12 we see that the total number of quarantined individuals
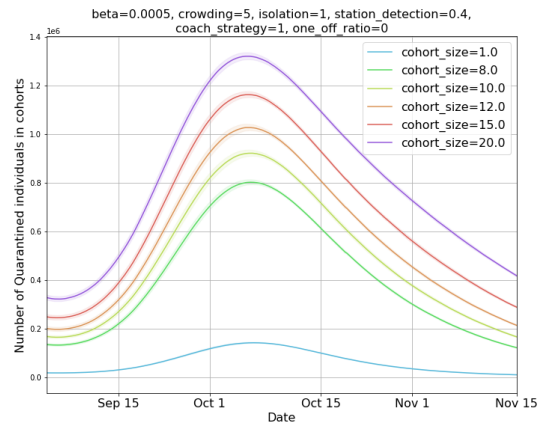
increases with increased cohort size, but the increase is quite modest. But in Figure 13 we see that the number of people quarantined due to cohorting increases quite substantially with increased cohort sizes, and as previously observed in Figure 4 cohorting with reasonable cohort size can reduce the daily positive cases substantially, and stem disease progresion. This tells us that cohorting is able to quarantine individuals even before testing, and contact tracing mechanisms kick in.

4 MODELING DETAILS

Once the cohort assignments are done, the simulator proceeds in 6hr timesteps. The simulator is seeded with 100 infected individuals at the start of the simulation. The time of seeding is chosen such that the fatalities observed in the simulator is in agreement with the fatalities observed in Mumbai at the start of the pandemic (fatalities increased from 10 to 200 during this period). The time of seeding is obtained as part of the simulator calibration step; we discuss in more detail in Section 4.1. At time step t, a susceptible individual n is exposed to a daily disease transmission rate $\lambda_n(t)$. The computation of $\lambda_n(t)$ takes into account the individual's interactions in all the interaction spaces he is associated with. The strength of interactions between an individual and the various interaction spaces are determined by the intervention policy active at the given time step. The intervention policies are chosen based on the announced policies. Some parameters (e.g., compliance parameter, contact tracing parameters) are tuned so that the simulator output is in reasonable agreement with the actual data from the city.

Given the daily disease transmission rate seen by an individual, the probability that the individual will become infected at the current timestep is modelled as $(1 - exp(-\lambda_n(t) \times \Delta_t))$, where $\Delta_t = 6/24$ is the duration of a timestep in days. Thus, computation of $\lambda_n(t)$ for every individual at every timestep is a key component of the simulator. For more details on how $\lambda_n(t)$ is computed, please see Section IV in [9].

In this study, we introduce cohorts and model the contribution from trains to an individual's transmission rate. Contribution from trains is modelled in two parts: 1) contribution from the same cohort, which we call the intra-cohort interaction, and from other cohorts that shares its journey with an individual's cohort, which we call the inter-cohort interactions. For cohort i, the intra-cohort transmission rate is modelled as

$$\lambda_{intra\_cohort}(i, t) = \sum_{n':Co(n')=i} \beta_{cohort} I_{n'}(t) \rho_{n'}(t) \kappa_w(n', t), \quad (1)$$

where the summation is across all individuals n' who belong to cohort i. $Co(n')$ denotes the individual to cohort mapping. $I_{n'}(t)$ denotes whether individual n' is infective at time t, $\rho_{n'}(t)$ is the infectiousness factor for individual n', and $\kappa_w(n', t)$ is a modulation factor for all workplace related interactions for individual n'. β_{cohort} denotes the transmission rate parameter, that can be used to calibrate the simulator behavior with actual observations.

The inter-cohort interaction seen by cohort i is modelled as

$$\lambda_{inter\_cohort}(i, t) = \sum_{j} \lambda_{intra\_cohort}(j, t) OT(i, j, t), \quad (2)$$

where j denotes all other cohorts and $OT(i, j, t)$ denotes the overlap time in the journeys of cohorts i and j, where two cohorts are considered to overlap only if they share a coach.

Once the intra-cohort and inter-cohort transmission rates are computed, the contribution of trains to a susceptible individual n's transmission rate is modelled as

$$\lambda_n^{trains}(t) = (\lambda_{intra\_cohort}(i, t) commute\_time(i) + \lambda_{inter\_cohort}(i, t)) \kappa_w(n, t), \quad (3)$$

where i denotes individual n's cohort, and $\kappa_w(n, t)$ is the workplace modulation factor for individual n.

In (3) we have assumed that, inside a coach, the interactions are homogeneous among all individuals in the coach. This assumption can be translated to uniform mixing of individuals in a coach. Even though we can expect cohort members to stay together and hence restrict interactions with other cohorts, the above assumption models the worst case scenario. The assumption is further reasonable as it will be difficult to implement physical distancing between cohorts and also to model the level of interactions between cohorts.

For cohorts, unlike the modelling of infection spread in other interaction spaces where we assume that the number of interactions of an individual remains constant for a given time interval [9], we assume that the number of interactions increases in proportion to the number of individuals traveling in a coach. We assume a linear increase in interactions as the number of individuals increase, though one could consider other alternatives like a monotonically increasing concave function.

4.1 Calibration of parameters

Like β_{coach} there are other tunable parameters in the simulator and it is important to tune the parameters to appropriate values to obtain reasonable outputs and insights from the simulator. We perform calibration in two steps. We seed a fixed number of individuals (100 in our case) in exposed state at the start of the simulation, and simulate a *no-intervention* (no mitigation strategies are enabled) scenario. We then tune the transmission parameters for home, workplace and community ($\beta_H, \beta_W, \beta_C$) to minimise the difference in slopes of the log of cumulative fatalities seen in the simulator to that of the actual cumulative fatalities observed in India between 26 March 2020 and 10 April 2020 (from 10 fatalities to 199 fatalities). We consider the *no-intervention* policy for calibration as the fatalities before April 10 2020 can be assumed to have got infected prior to imposition of any restrictions in India. A linear fit for the log fatalities curve is based on the assumption that cumulative fatalities grow exponentially with time, which was observed to be consistent with actual data. We observe a good match in the slopes of the fatalities curves for India and Mumbai, suggesting similar disease transmission rates in Mumbai and in the whole of India in the initial days of the pandemic.

Transmission parameters in interaction spaces are tied to one of the above three parameters. For example, we assume that the transmission parameter for a project team is nine times that of the transmission parameter for the larger workplace. This is based on the assumption that an individual spends 90% of the time in office with their team members and only the remaining 10% with the larger workplace group. We further try to equalise the contribution

of household, workplace and community towards disease spread. We use *stochastic approximation* methods to arrive at the appropriate parameters values. Once we match the growth rate of fatalities, we calibrate the start of simulation date with the actual fatalities timeline, so that the time series of fatalities of the simulator matches in expectation with the actual data.

4.1.1 Calibration of β_{coach}. Due to sparsity of data on the impact of trains on disease transmission we have not been able to calibrate β_{coach} independently. We use the following heuristic argument to compute a nominal β_{coach} from β_H, where β_H is the transmission rate parameter associated with households.

The infection transmission rate seen by an individual n from their household at time t is modeled as

$$\lambda_n^H(t) = \beta_H \frac{1}{n_H^\alpha} \sum_{n'=1}^{n_H} I_{n'}(t) \rho_{n'}(t) \kappa_H(n', t), \qquad (4)$$

where the summation is across all individuals in the household, $(1 - \alpha)$ denotes the crowding factor for households, $I_{n'}(t)$ denotes whether individual n' is infective at time t, $\rho_{n'}(t)$ denotes individual n''s infectiousness factor and $\kappa_H(n', t)$ denotes individual n''s household based modulation factor.

Thus, β_H can be interpreted as the household transmission rate per day for an individual. Let r_H denote the number of typical contacts for an individual at home for a day. Then, the probability of transmission from a contact can modeled as $p_c = \frac{\beta_H}{r_H}$.

Let the number of typical contacts per minute per individual in a train coach be r_T. Then, the effective transmission rate per minute per individual in coach, $\hat{\beta}_{coach}$, can be expressed in terms of r_T as

$$\hat{\beta}_{coach} = p_c r_T = \frac{\beta_H r_T}{r_H}. \qquad (5)$$

If we assume that the number of close contacts per day in a household $r_H = 50$ contacts per day, and close contacts per minute per individual in a coach $r_T = 1/100$, $\hat{\beta}_{coach}$ can be computed in terms of β_H as:

$$\hat{\beta}_{coach} = \beta_H \frac{r_T}{r_H} = \beta_H \frac{1}{100} \frac{1}{50} = \beta_H 0.0002. \qquad (6)$$

In the simulator, for every simulation timestep Δ_t, the transmission rate is further multiplied by Δ_t to obtain the mean disease transmitting contacts per simulation timestep. For trains, since we already account for commute time, and since we assume that one journey is restricted to one simulation time step, we need to discount the further multiplication by Δ_t. Thus, a nominal value for the β_{coach} parameter we use in simulator, in terms of β_H can be obtained as

$$\beta_{coach} = \frac{\hat{\beta}_{coach}}{\Delta_t} = \hat{\beta}_{coach} 4 = \beta_H 0.0008, \qquad (7)$$

where we have used $\Delta_t = 1/4$ days, to account for a simulation timestep duration of 6hrs.

4.2 Intervention Modelling

A key feature of the simulator in [9] is its ability to simulate various intervention strategies. The simulator has the ability to model various intervention strategies via a file interface, that in turn modulates the individual's edge weight with an interaction space. For example, when an individual is self-isolated at home, contact rates with their household is reduced by 25%, contact rates with their workplace is reduced to zero and contact rates with the community is reduced to 10%. The simulator also supports testing and contact tracing protocols. Contact tracing in the close network of an individual can be initiated for each of the following events: 1) an individual is hospitalised, 2) an individual tests positive, 3) an individual turns symptomatic. The fraction of such events that trigger contact tracing and the fraction of individuals who would be contact traced are all configurable.

For this particular study on Mumbai, we consider a pre-lockdown period starting from March 16 and extending till May 18 in Mumbai. Post May 18, we assume a phased re-opening of offices, with 5% offices operating till May 31, followed by 15% attendance till June 30, followed by 25% attendance till July 31, followed by 33% attendance till Aug 31 and 50% attendance thereafter. Further, We assume masks were enforced from April 09. Compliance probabilities to the regulations (including mask wearing) are 40% in high density areas and 40% in high density areas. Trains are assumed to re-start from September 07.

4.3 Intervention Modelling - Cohorts

In the specific case of cohorts, we study the impact of isolating an entire cohort when an individual is hospitalised or tested positive or is sufficiently symptomatic. When an individual is hospitalised or tested positive, then all their cohort members are placed under self isolation. A symptomatic individual may self-declare or be detected at a station and that can also trigger isolation of the other cohort members.

In Table 1, we list the common parameter values used in the simulator. For a detailed description on each of these parameters, please refer Section IV in [9].

5 RELATED WORK

The literature on agent-based models (ABMs) is vast, see for example [3, 4, 8] (ABM frameworks), [10] (modeling of small pox spread), [14] (benefit of fine-grained model), [1, 6] (fine-grained modeling of slums in Delhi and influenza spread), [26] (benefit of using auxiliary data sources for modeling Ebola spread), [23] (use of survey data to model behaviour), [2, 25, 27] (time-varying graph networks), [22] (vaccination), [24] (ABMs for computational epidemiology), [17, 20] (review of epidemic spread in complex networks) and [28] (impact of mobility on COVID-19 spread).

We shall focus only on those closely related to our work in this paper. Mei et al. [18] developed a city-scale ABM for Beijing (6M agents) using detailed demographic, mobility, socio-economic data. The data they needed are quite detailed, the interventions modeled have limited flexibility, and the test-isolate strategy is not modeled. Cooley et al. [7] developed a city-scale ABM (7.5M agents) based on survey data to study H1N1 epidemic spread in the New York City. They calibrated the parameters based on the 1957-8 influenza

Table 1: Model parameters

Parameter	Symbol	Mumbai
Transmission coefficient at home	β_h	0.7928 (calibrated)
Transmission coefficient at school	β_s	0.2834 (calibrated)
Transmission coefficient at workplace	β_w	0.1417 (calibrated)
Transmission coefficient at community	β_c	0.0149 (calibrated)
Subnetwork upscale factor	$\tilde{\beta}$	9
Transmission coefficient at transport space	β_{cohort}	0.0005
Household crowding	$1 - \alpha$	0.2
Community crowding	r_c	2
Distance kernel $f(d) = 1/(1 + (d/a)^b)$	(a, b)	(2.709, 1.279)
Infectiousness shape (Gamma distributed)	(shape,scale)	(0.25, 4)
Severity probability	$\Pr\{C_n = 1\}$	0.5
Age stratification	$M_{n,n'}$	Not used
Project subnetwork size range	$n_{\mathscr{W}(n)}$	$3 - 10$
Family friends' subnetwork range	no symbol	2-5 families

spread data. The interventions are limited to wearing masks, vaccinations and social distancing. They conclude that interventions targeting the subway system alone are not sufficiently effective in mitigating the infection spread. The papers [11, 13, 15] use a density model developed in [12] for narrow and enclosed areas to study the correlation between mobility and infection spread in crowded spaces. The validation of these models are limited to statistical data analysis [15] and small-scale simulations (200 – 100,000 agents) [12, 13]. Social bubbles have been studied by [16, 19, 21] using ABMs. However, these ABMs are modeled with limited interaction spaces [16], or do not consider local demographic variations [21], or limit the number of agents to about 100,000 [5].

In this work, we overcome several of the limitations highlighted above. We model the interactions more realistically by considering multiple and hierarchical interactions spaces like homes, neighbourhoods, communities, schools, and workplaces, in addition to interactions during commute. Our simulator works with 12.4M agents. The contact rate parameters are calibrated to the COVID-19 India data. The simulator enables time-varying interventions that model on-ground policies (containment zones, lockdown fatigue, compliance, contact tracing policies, and quarantine duration). Additionally, the simulator implements the test-isolate strategy.

REFERENCES

[1] Abhijin Adiga, Shuyu Chu, Stephen Eubank, Christopher J Kuhlman, Bryan Lewis, Achla Marathe, Madhav Marathe, Eric K Nordberg, Samarth Swarup, Anil Vullikanti, et al. 2018. Disparities in spread and control of influenza in slums of Delhi: findings from an agent-based modelling study. *BMJ open* 8, 1 (2018).

[2] Alessia Antelmi, Gennaro Cordasco, Carmine Spagnuolo, and Vittorio Scarano. 2020. A Design-Methodology for Epidemic Dynamics via Time-Varying Hypergraphs. In *Proceedings of the 19th International Conference on Autonomous Agents and MultiAgent Systems (AAMAS' 20)*. 61–69.

[3] Michael Balmer, Konrad Meister, Marcel Rieser, Kai Nagel, and Kay W Axhausen. 2008. Agent-based simulation of travel demand: Structure and computational performance of MATSim-T. *Arbeitsberichte Verkehrs-und Raumplanung* 504 (2008).

[4] Christopher L Barrett, Keith R Bisset, Stephen G Eubank, Xizhou Feng, and Madhav V Marathe. 2008. EpiSimdemics: an efficient algorithm for simulating the spread of infectious disease over large realistic social networks. In *SC'08: Proceedings of the 2008 ACM/IEEE Conference on Supercomputing*. IEEE, 1–12.

[5] Per Block, Marion Hoffman, Isabel J Raabe, Jennifer Beam Dowd, Charles Rahal, Ridhi Kashyap, and Melinda C Mills. 2020. Social network-based distancing strategies to flatten the COVID-19 curve in a post-lockdown world. *Nature Human Behaviour* (2020), 1–9.

[6] Jiangzhuo Chen, Shuyu Chu, Youngyun Chungbaek, Maleq Khan, Christopher Kuhlman, Achla Marathe, Henning Mortveit, Anil Vullikanti, and Dawen Xie. 2016. Effect of modelling slum populations on influenza spread in Delhi. *BMJ open* 6, 9 (2016).

[7] Philip Cooley, Shawn Brown, James Cajka, Bernadette Chasteen, Laxminarayana Ganapathi, John Grefenstette, Craig R Hollingsworth, Bruce Y Lee, Burton Levine, William D Wheaton, et al. 2011. The role of subway travel in an influenza epidemic: a New York City simulation. *Journal of urban health* 88, 5 (2011), 982.

[8] Sara Y Del Valle, Phillip D Stroud, James P Smith, Susan M Mniszewski, Jane M Riese, Stephen J Sydoriak, and Deborah A Kubicek. 2006. EpiSimS: epidemic simulation system. *Los Alamos, NM: Los Alamos National Laboratory* (2006).

[9] Shubhada Agrawal et.al. 2020. City-Scale Agent-Based Simulators for the Study of Non-Pharmaceutical Interventions in the Context of the COVID-19 Epidemic. arXiv:2008.04849 [q-bio.PE]

[10] Stephen Eubank, Hasan Guclu, VS Anil Kumar, Madhav V Marathe, Aravind Srinivasan, Zoltan Toroczkai, and Nan Wang. 2004. Modelling disease outbreaks in realistic urban social networks. *Nature* 429, 6988 (2004), 180–184.

[11] Edward L Glaeser, Caitlin S Gorback, and Stephen J Redding. 2020. *How much does covid-19 increase with mobility? evidence from new york and four other us cities*. Technical Report. National Bureau of Economic Research.

[12] Lara Goscé, David AW Barton, and Anders Johansson. 2014. Analytical modelling of the spread of disease in confined and crowded spaces. *Scientific reports* 4 (2014), 4856.

[13] Lara Goscé and Anders Johansson. 2018. Analysing the link between public transport use and airborne transmission: mobility and contagion in the London underground. *Environmental Health* 17, 1 (2018), 84.

[14] Jürgen Hackl and Thibaut Dubernet. 2019. Epidemic spreading in urban areas using agent-based transportation models. *Future Internet* 11, 4 (2019), 92.

[15] Jeffrey E Harris. 2020. The subways seeded the massive coronavirus epidemic in new york city. *NBER Working Paper* w27021 (2020).

[16] Trystan Leng, Connor Whie, Joe Hilton, Adam J Kucharski, Lorenzo J Pellis, Helena Stage, Nicholas G Davies, Matt J Keeling, and Stefan Flasche. 2020. The effectiveness of social bubbles as part of a Covid-19 lockdown exit strategy, a modelling study. *medRxiv* (2020).

[17] Madhav Marathe and Anil Kumar S Vullikanti. 2013. Computational epidemiology. *Commun. ACM* 56, 7 (2013), 88–96.

[18] Shan Mei, Bin Chen, Yifan Zhu, Michael Harold Lees, AV Boukhanovsky, and Peter MA Sloot. 2015. Simulating city-level airborne infectious diseases. *Computers, Environment and Urban Systems* 51 (2015), 97–105.

[19] Bjarke Frost Nielsen and Kim Sneppen. 2020. COVID-19 superspreading suggests mitigation by social network modulation. *medRxiv* (2020).

[20] Romualdo Pastor-Satorras, Claudio Castellano, Piet Van Mieghem, and Alessandro Vespignani. 2015. Epidemic processes in complex networks. *Reviews of modern physics* 87, 3 (2015), 925.

[21] Jose Paulo Guedes Pinto, Patricia Camargo Magalhaes, Gerusa Maria Figueiredo, Domingos Alves, and Diana Maritza Segura-Angel. 2020. Local protection bubbles: an interpretation of the decrease in the velocity of coronavirus's spread in the city of Sao Paulo. *medRxiv* (2020).

[22] Prathyush Sambaturu, Bijaya Adhikari, B Aditya Prakash, Srinivasan Venkatramanan, and Anil Vullikanti. 2020. Designing Effective and Practical Interventions

to Contain Epidemics. In *Proceedings of the 19th International Conference on Autonomous Agents and MultiAgent Systems (AAMAS' 20)*. International Foundation for Autonomous Agents and Multiagent Systems, Richland, SC, 1187–1195.

[23] Meghendra Singh, Achla Marathe, Madhav V Marathe, and Samarth Swarup. 2018. Behavior model calibration for epidemic simulations. In *Proceedings of the 17th International Conference on Autonomous Agents and MultiAgent Systems (AAMAS' 18)*. International Foundation for Autonomous Agents and Multiagent Systems, Richland, SC, 1640–1648.

[24] Samarth Swarup, Stephen G Eubank, and Madhav V Marathe. 2014. Computational epidemiology as a challenge domain for multiagent systems. In *Proceedings of the 2014 international conference on Autonomous agents and MultiAgent systems (AAMAS' 14)*. International Foundation for Autonomous Agents and Multiagent Systems, Richland, SC, 1173–1176.

[25] Michele Tizzani, Simone Lenti, Enrico Ubaldi, Alessandro Vezzani, Claudio Castellano, and Raffaella Burioni. 2018. Epidemic spreading and aging in temporal networks with memory. *Physical Review E* 98, 6 (2018), 062315.

[26] Srinivasan Venkatramanan, Bryan Lewis, Jiangzhuo Chen, Dave Higdon, Anil Vullikanti, and Madhav Marathe. 2018. Using data-driven agent-based models for forecasting emerging infectious diseases. *Epidemics* 22 (2018), 43–49.

[27] Christian L Vestergaard and Mathieu Génois. 2015. Temporal gillespie algorithm: Fast simulation of contagion processes on time-varying networks. *PLoS Comput Biol* 11, 10 (2015), e1004579.

[28] Ding Wang, Brian Yueshuai He, Jingqin Gao, Joseph YJ Chow, Kaan Ozbay, and Shri Iyer. 2020. Impact of COVID-19 Behavioral Inertia on Reopening Strategies for New York City Transit. arXiv:2006.13368